Vibrational inelastic scattering effects in molecular electronics

H Ness * and A J Fisher #
* CEA-Saclay, Service de Physique et de Chimie des Surfaces
et Interfaces, DSM/DRECAM, Bât 462, 91191 Gif sur Yvette,
France, ness@dsm-mail.saclay.cea.fr;
Department of Physics and Astronomy and
London Centre for Nanotechnology,
University College London, Gower Street,
London WC1E 6BT, UK, andrew.fisher@ucl.ac.uk

February 6, 2008

Abstract

We describe how to treat the interaction of travelling electrons with localised vibrational modes in nanojunctions. We present a multichannel scattering technique which can be applied to calculate the transport properties for realistic systems, and show how it is related to other methods that are useful in particular cases. We apply our technique to describe recent experiments on the conductance through molecular junctions.

.

Introduction

Electronic transport through nanoscale systems connected to external electrodes exhibits a number of new features when compared to conduction through macroscopic systems. Primary among these is the importance of local interactions–including Coulomb interactions between the electrons, and scattering from localised atomic vibrations. Crudely speaking these effects are more important in nanoscale systems because the electronic probability density is concentrated in a small region of space; normal screening mechanisms are then ineffective.

Perhaps the most extreme instance of nanoscale transport is where an electrical connection is formed through a single molecule. This paper describes how to approach electron transport in such systems theoretically. Our aim is to convince the reader that in many cases the local interaction is not a small perturbation which can be added in later—instead, it plays the principal role in determining the transport physics. In order to treat it, we need to understand the role of the local molecular properties—dominated by these local interactions—in scattering current-carrying electrons as they pass by. As well as determining the current flow, the interactions are then responsible for other important phenomena such as local heating.

Such a situation is already familiar in the physics of transport through semiconductor quantum dots [1], where local Coulomb interactions produce Coulomb blockade (regions of very low conductance where changes in the charge state of the dot are energetically forbidden) and the Kondo effect (where the local spin of the dot electrons is screened by the conducting carriers). But the situation in molecules, where the length scales are smaller and the electronic energy scales are correspondingly larger, is only now being studied.

If the (three-dimensional) extent of an electronic wavepacket is L, the Coulomb interaction between electrons scales as L^{-1}, while the energy arising from short-range interactions with lattice vibrations scales as L^{-3} [2]. We might therefore expect the electron-lattice interactions to

dominate for single molecules where L is small, and indeed their signatures have been observed in several recent experiments with single molecules (or small numbers) [3, 4, 5, 6]. These experiments include inelastic electron tunneling spectroscopy (IETS) of small molecules adsorbed on surfaces [3], studies of molecular-scale transistors [4], and experiments on molecular junctions made of alkyl or π-conjugated molecular wires [5] or alkanedithiol self-assembled monolayers [6]. Such experiments show the possibility of exciting specific vibrational modes by injecting electrons; these excitations show up as sharp features in the differential conductance.

It has been known for many years that coupling between electrons and molecular vibrations plays an important role in transport properties of bulk films of long conjugated molecules (such as conducting and semiconducting polymers); the transport then occurs by classical diffusion of polarons or solitons [8]. The new realisation is that such effects are also crucial in nanoscale transport through individual molecules, even although a classical diffusive model for the resulting composite excitations is no longer appropriate. This new realisation has coincided with an appreciation of the importance of local heating [11], another manifestation of the coupling between electrons and phonons.

Corresponding to this experimental progress, theorists have increasingly been studying electron transport in the presence of local electron-phonon (e-ph) coupling in the molecule. In cases where the e-ph effects are weak (for example, in IETS of small molecules, where the electron residence time on the molecule is very short), perturbation theory for the e-ph interaction can be used to interpret IETS spectra for model systems [9] and for more realistic systems including small molecules on surfaces [10] and molecular wires [12]. Going beyond perturbative approximations, the effects of e-ph coupling have been considered using scattering theory and Green's functions approaches [13, 14, 15, 16, 17, 18, 19], using master and kinetic equations [20], and reduced density matrix approaches [21]. Another contribution including dissipation with a semiclassical treatment of the vibration was also developped [22]. More recently, approaches based on non equilibrium statistical physics have been developped for model systems [23, 24] and realistic atomic and molecular wires [25, 26, 27].

In this paper, we describe the effects of the coupling between injected electrons and molecular vibrations (both treated on the quantum level) by using a multi-channel inelastic scattering technique. We show that it is important to treat such local interactions non-perturbatively, and how our approach relates to others. In the final part we study the effects of the temperature on the conductance properties and shed some light on the basic understanding of the features observed in IETS spectra.

Note that in the following, we consider independent charge carriers interacting with single or multiple quantized vibrational modes. Calculations including the interaction between charges [28] or the interaction between charge and classical vibrations [29] have been considered elsewhere.

Model

Before presenting some numerical results, we describe our approach to inelastic transport and its relation to other approaches.

Physical model

Our model involves those delocalized electron states which simultaneously carry current through the molecule and interact with its eigenmodes of vibration. In the case of conjugated molecules these states are predominantly derived from the π orbitals (though our method can deal equally with other types of state, and there are no restrictions on the geometry or dimensionality). If the molecular vibrations are approximately harmonic, the reference Hamiltonian H_0 for the molecule is

$$H_0 = H_{\rm el} + \sum_\lambda \omega_\lambda a_\lambda^\dagger a_\lambda \tag{1}$$

where $H_{\rm el}$ is the purely electronic Hamiltonian and λ labels the eigenmodes of vibration of the isolated molecule in its equilibrium (generally neutral) charge state; $a_\lambda^\dagger$ creates (a_λ annihilates) a quantum of energy ω_λ in mode λ. Note that $H_{\rm el}$ may, in principle, contain electron-electron interactions.

Our fundamental approximation is to consider the scattering only of *single* electrons or holes from the molecule. We expect this assumption to be reasonable when the interval between carrier transmission events is much greater than the transit time through the molecule [17], and provided that the applied bias does not cause significant fluctuations in the occupancy of the molecular eigenstates (i.e. provided one charge state of the molecule dominates during the transport process).

For electron transport, if the equilibrium charge state contains N electrons and $|0,N\rangle$ is the N-electron ground state, we construct an electronic basis $|i,N+1\rangle = c_i^\dagger|0,N\rangle$ where the $\{c_i^\dagger\}$ create an electron in a sufficiently complete set of orbitals (for example, in all the low-lying π-states of the molecule). For hole transport we would use $|j,N-1\rangle = c_j|0,N\rangle$. We now diagonalize $H_{\rm el}$ (keeping the phonon coordinates fixed, for the moment) within our restricted $(N\pm1)$-electron basis to obtain a set of approximate $(N\pm1)$-electron eigenstates. Using the electron creation ($c_n^\dagger$) and annihilation (c_n) operators and the energies ϵ_n, we can write

$$H_{\rm el} = \sum_n \epsilon_n c_n^\dagger c_n. \tag{2}$$

The approximate $(N\pm1)$-electron eigenstates of the full H_0 can thus be written as $|n,\{n_\lambda\}\rangle$, where n labels an electronic eigenstate and the $\{n_\lambda\}$ are occupation numbers for the vibrational modes:

$$|n,\{n_\lambda\}\rangle = c_n^\dagger \prod_\lambda (a_\lambda^\dagger)^{n_\lambda}/\sqrt{n_\lambda!}\;|0,N,\{0_\lambda\}\rangle \tag{3}$$

and $|0,N,\{0_\lambda\}\rangle$ is the electronic and vibrational ground state for N electrons.

The e-ph coupling term $H_{e\rm ph}$ is taken to be linear in the phonon displacements and induces transitions between these electronic states:

$$H_{e\rm ph} = \sum_{\lambda,n,m} \gamma_{\lambda nm}(a_\lambda^\dagger + a_\lambda)c_n^\dagger c_m\ . \tag{4}$$

The values of ϵ_n, ω_λ and $\gamma_{\lambda nm}$ are calculated from a suitable model of the isolated molecule. In our work on conjugated molecules [17] we have used the Su-Schrieffer-Heeger (SSH) [8] model within the harmonic limit.

To obtain the transport properties, we perform a thought experiment in which we connect the left and right ends of the molecule to metallic leads and scatter a single incoming charge carrier (electron or hole). The coupling matrix elements are $v_{L,R}$ respectively; since we do not wish to focus on the properties of the leads we take the simplest possible model for them and consider one-dimensional semi-infinite chains (with on-site energy $\epsilon_{L,R}$ and hopping integrals $\beta_{L,R}$, giving dispersion relations $\epsilon = \epsilon_{L,R} + 2\beta_{L,R}\cos(k_{L,R})$, where $k_{L,R}$ are dimensionless wavevectors). We assume transport is purely elastic within the leads themselves; dissipation occurs in remote reservoirs, as in the standard Landauer picture for electron transport. The scattering states $|\Psi\rangle$ for a single incoming carrier are then expanded inside the molecule onto the eigenstates $|n,\{n_\lambda\}\rangle$ of H_0. The single added carrier can be anywhere in the system and interacts with lattice vibrations only when inside the molecule.

The transport problem is solved by mapping the many body problem onto a single-electron one with many scattering channels [13, 15, 17]; each channel represents a process by which the electron might exchange energy with the vibration modes. For an initial mode distribution $b \equiv \{m_\lambda\}$ and an incoming electron from the left, the outgoing channels in the left and right leads are associated with energy-dependent reflection coefficients $r_{ab}(\epsilon)$ and transmission coefficients $t_{ab}(\epsilon)$, where $a \equiv \{n_\lambda\}$ is the final mode distribution. In the leads, the scattering states are propagating waves with amplitudes r_{ab} (reflection) and t_{ab} (transmission), and wave vectors

corresponding to the initial ($\epsilon_{\rm in}$) and final ($\epsilon_{\rm fin}$) electronic energies. By projecting out the leads, we work entirely in the molecular subspace to obtain the scattering state $|\Psi\rangle$ by solving

$$\begin{aligned}[\omega - H_0 - H_{e\rm ph} - \Sigma_L^r(\omega) - \Sigma_R^r(\omega)]\ |\Psi(\omega)\rangle \\ \equiv G^r(\omega)^{-1}|\Psi(\omega)\rangle = |s_b(\omega)\rangle.\end{aligned} \tag{5}$$

Here ω is the conserved total energy;

$$\omega = \epsilon_{\rm in} + \sum_\lambda m_\lambda \omega_\lambda = \epsilon_{\rm fin} + \sum_\lambda n_\lambda \omega_\lambda. \tag{6}$$

The source term $|s_b(\omega)\rangle$ is fixed by the incoming boundary conditions, while $\Sigma^r_{L,R}(\omega)$ are the electron self-energies arising from the coupling of the molecule to the leads. The components of the scattering states then give the matrix elements of the retarded Green's function $G^r(\omega)$. In practice, the linear system $|\Psi\rangle = G^r|s\rangle$ is solved for a finite-size molecular subspace, by truncating the occupation number above a maximum $n_\lambda^{\rm max}$ in each mode. This is physically reasonable because the injected charge cannot populate infinitely many excitations.

From the solution of Eq.(5), we can calculate any observable property, such as the expectation value of an operator A: $\langle A\rangle = \sum_{\{b\}} \mathcal{W}_b^{\rm ph}(T)\langle\Psi|A|\Psi\rangle$ where $\mathcal{W}_b^{\rm ph}(T)$ is the statistical weight of the distribution $b \equiv \{m_\lambda\}$ of modes at temperature T. The transmission probability T_{ab} is given from the square of the transmission coefficients t_{ab} with the usual ratio of the electron velocities in the outgoing and incoming channels. In our model, $t_{ab} \propto \langle i = N|G_{ab}|s\rangle$ and the transmission probability T_{ab} is written as [18, 19]

$$\begin{aligned}T_{ab}(\epsilon_{\rm fin},\epsilon_{\rm in}) = 4\ \frac{v_L^2}{\beta_L}\sin k_b^L(\epsilon_{\rm in})\ \frac{v_R^2}{\beta_R}\sin k_a^R(\epsilon_{\rm fin}) \\ \times|\langle i = N|G^r_{ab}(\omega)|i = 1\rangle|^2\ ,\end{aligned} \tag{7}$$

where $\langle N|G^r_{ab}(\omega)|1\rangle$ is the matrix element of the Green's function G^r taken between the left side $i = 1$ and the right side $i = N$ of the molecule and the vibration distributions before (b) and after (a) scattering. The factors $v^2_{L,R}/\beta_{L,R}\sin k^{L,R}_{b,a}$ are related to the imaginary parts of the retarded self-energies $\Sigma^r_{L,R}$.

Two concluding notes are in order. First, this procedure solves the problem *non-perturbatively* in the e-ph interaction. Second, we have described the method for the case where the channel structure of the leads is generated only by the vibrational excitations of the molecule, but it is straightforward to generalise it to the case of multiple spatial channels in the leads.

Connection to other methods

Here we etablish how the multichannel scattering technique is related to other methods based on two-particle Green's functions for non-interacting electrons [31] and on non-equilibrium Green's functions [24, 25, 26, 27]. We will show below (for a simplified molecular model) that G^r can be reformulated to include the self-energies arising from the coupling of the molecule to the leads ($\Sigma^r_{\rm leads}$) and from the interaction of the electron with the vibrations ($\Sigma^r_{e\rm ph}$).

Let us start with the generalisation of the Landauer formula for non-equilibrium interacting systems given in Ref.[32]. In the following we consider the single-site, single-vibrational mode (SSSM) model, which allows us to illustrate the essential physics without complicating the algebra. We first assume that the left and right leads are identical, and couple to the molecule via energy-independent hopping integrals. Then, the self-energies $\Sigma^r_{L,R}$ (and their imaginary parts $\Gamma_{L,R}$) are proportional to each other. According to Ref.[32], the current through the junction is then given by

$$I = \frac{2e}{h}\int d\omega\,(f_L(\omega) - f_R(\omega))\,{\rm Im Tr}\{\Gamma(\omega)G^r(\omega)\}\ , \tag{8}$$

where $f_{L,R}$ is the Fermi distribution of the left and right (non-interacting) lead respectively, $\Gamma \equiv \Gamma_L\Gamma_R/(\Gamma_L + \Gamma_R)$ and G^r is the retarded Green's function of the molecule including the

self-energies arising from the coupling to the leads and from the interaction between particles. Here we consider non-interacting charge carriers coupled to vibrations of the molecule.

Within the SSSM model there is only one energy level ϵ_0 that couples to a single mode of frequency ω_0 with a coupling constant γ_0. For this model, G^r is the inverse of a tridiagonal matrix R in the subspace $|\chi_n\rangle$ of the excitations n of the vibrational mode ($n = 0$ is ground state of the mode) with diagonal elements $R_{n,n} = \omega - \epsilon_0 - n\omega_0 - \Sigma^r_{\{n\}}(\omega)$ and non-zero off-diagonal elements $R_{n,n+1} = -\gamma_0\sqrt{n+1}$ and $R_{n,n-1} = -\gamma_0\sqrt{n}$. Here $\Sigma^r_{\{n\}}(\omega)$ is the retarded self-energy of both leads for the channel containing n phonon excitations; it is calculated by taking into account the energy conservation condition Eq.(6), which reduces in the limit of very low temperature to $\omega = \epsilon_{in} = \epsilon_{fin} + n\omega_0$. Furthermore, in this limit, only the matrix element of G^r between the phonon ground state $G^r_{00} = \langle\chi_0|G^r(\omega)|\chi_0\rangle$ enters in the evaluation of the current. It can be expressed as a continued fraction:

$$\begin{aligned} G^r_{00}(\omega) = [\omega - \epsilon_0 - \Sigma^r_{\{0\}}(\omega) - \\ \gamma_0^2/(\omega - \epsilon_0 - \omega_0 - \Sigma^r_{\{1\}}(\omega) - \\ 2\ \gamma_0^2/(\omega - \epsilon_0 - 2\omega_0 - \Sigma^r_{\{2\}}(\omega) - \\ 3\ \gamma_0^2/(\omega - \epsilon_0 - 3\omega_0 - \Sigma^r_{\{3\}}(\omega) - ...]^{-1} \end{aligned} \tag{9}$$

The imaginary part of G^r_{00} can be rewritten as the sum of several terms:

$$\begin{aligned} \mathrm{Im}G^r_{00}(\omega) = |G^r_{00}(\omega)|^2\ \times \\ \mathrm{Im}\left\{\Sigma_{\{0\}} + \frac{\gamma_0^2}{\omega - \epsilon_0 - \omega_0 - \Sigma^r_{\{1\}} - ...}\right\}\ . \end{aligned} \tag{10}$$

After some calculation, it can be shown that $\mathrm{Im}G^r_{00}$ is actually related to the other non-diagonal elements $\langle\chi_n|G^r|\chi_0\rangle$ of the Green's function and that finally one has

$$\mathrm{Im}\langle\chi_0|G^r|\chi_0\rangle = \sum_n \mathrm{Im}\Sigma^r_{\{n\}}\ |\langle\chi_n|G^r|\chi_0\rangle|^2\ . \tag{11}$$

Introducing this result in Eq.(8), the current for the SSSM model is then expressed as the sum of the elastic and inelastic transmission probabilities $T_{ab}(\epsilon', \epsilon)$ obtained from Eq.(7).

One can perform a similar derivation at a finite temperature T. The current is then determined from all the diagonal matrix elements Im $\langle\chi_n|G^r|\chi_n\rangle$ including the appropriate statistical weight $\mathcal{W}^{\mathrm{ph}}_n(T)$ for the n-th excitation of the vibration mode. Each matrix element Im $\langle\chi_n|G^r|\chi_n\rangle$ is related to the sum of the elastic and inelastic transmission coefficients where the vibration mode is in the n-th excited state before scattering, and in the m-th excited state afterwards.

The derivations given above can be extended to general cases in which many electronic levels are coupled to many vibration modes. Then the R matrix which defines G^r is block-tridiagonal; the diagonal blocks correspond to purely electronic processes with constant phonon occupancy, while the off-diagonal blocks correspond to the e-ph coupling matrix $\gamma_{\lambda nm}$. The equivalent matrix element $\langle\{0_\lambda\}|G^r|\{0_\lambda\}\rangle$ of Eq.(9) is then written as a matrix continued fraction in the corresponding basis. The same reasoning derived above holds for calculating the current in terms elastic and inelastic transmission probabilities T_{ab} for all temperatures.

Now, we show how to connect Eq.(11) to the approach developed in [31]. For this, let us consider the wide-band limit for the leads, so the lead self-energies become independent of the energy and hence of the channel considered, and are purely imaginary $\Sigma^r_n(\omega) \equiv\ i\Gamma = i(\Gamma_L + \Gamma_R)$. The imaginary part of G^r_{00} then becomes Im $G^r_{00}(\omega) = \Gamma\sum_n |\langle\chi_n|G^r|\chi_0\rangle|^2$. It is convenient to work in this limit to circumvent the problems of band-width renormalisation when one introduces the transformation U that diagonalises $H = H_0 + H_{\mathrm{eph}} = \epsilon_0 c_0^\dagger c_0 + \omega_0 a_0^\dagger a_0 + \gamma_0(a_0^\dagger + a_0)c_0^\dagger c_0$. We introduce the basis set $|\tilde{\chi}_n\rangle = U|\chi_n\rangle$, and obtain

$$\mathrm{Im}\ G^r_{00} = \Gamma\sum_n \left|\sum_l \frac{\langle\chi_n|\tilde{\chi}_l\rangle\langle\tilde{\chi}_l|\chi_0\rangle}{\omega - \tilde{\epsilon}_0 - l\omega_0 + i\Gamma}\right|^2\ , \tag{12}$$

where $\tilde{\epsilon}_0 = \epsilon_0 - g^2\omega_0$ and $g = \gamma_0/\omega_0$. Then, calculating the overlaps $\langle\chi_n|\tilde{\chi}_l\rangle$ between the original $|\chi_n\rangle$ and displaced harmonic states $|\tilde{\chi}_n\rangle$ as in [30], one ultimately finds

$$\text{Im } G^r_{00}(\omega) = \Gamma e^{-2g^2} \sum_{n=0}^{\infty} \frac{g^{2n}}{n!} \times \left| \sum_{j=0}^{n} (-1)^j \binom{n}{j} \sum_{l=0}^{\infty} \frac{g^{2l}}{l!} \frac{1}{\omega - \tilde{\epsilon}_0 - (j+l)\omega_0 + i\Gamma} \right|^2 \tag{13}$$

Eq.(13) is just the result derived in [31] for the transmission by starting from a two-particle Green's function description for a single resonant level coupled to a single vibration mode.

It should be noticed that the equivalence between the two approaches is only valid in the wide-band limit for which the full polaron shift is obtained (i.e., ϵ_0 shifted by the relaxation energy $-\gamma_0^2/\omega_0$). In other cases, the energy dependence of the self-energies $\Sigma^r_{\{n\}}$ plays an important role. Furthermore when the residence time of the electron in the molecule is not long enough for the vibration to respond fully to its presence, the full relaxation is not obtained and one has an intermediate polaron shift[1]. However there are no such limitations in the multichannel scattering technique, which can treat the problem for the full parameter range (including strong e-ph coupling)—provided only that the fundamental assumption of single-carrier transport (see the discussion following Eq.(1)) remains valid.

Finally, in this section, we show how the multichannel scattering technique is related to more recent approaches based on non-equilibrium Green's functions [23, 24, 25, 26, 27]. Such a non-equilibrium approach is more suitable when our assumption of a well-defined reference charge state breaks down. Let us first rewrite the retarded Green's function in Eq.(9) as

$$G^r(\omega) = [\omega - \epsilon_0 - \Sigma^r_{\{0\}}(\omega) - \Sigma^r_{\text{eph}}(\omega)]^{-1} \ , \tag{14}$$

where the self-energy due to the interaction between electron and phonon is *symbolically* and *recursively* given by $\Sigma^r_{\text{eph}}(\omega) \equiv \gamma_0^2 \ G^r(\omega - \omega_0)$ [2]. Note that by definition [17], one has the following relation for the lead self-energy: $\Sigma^r_{\{0\}}(\omega - n\omega_0) = \Sigma^r_{\{n\}}(\omega)$.

In a many-body non-equilibrium Green's functions approach, the self-energies arising from the interaction between particles are obtained from a diagrammatic perturbation expansion of the interaction and by applying the rules for the time ordering and for the evaluation of products of double-timed operators on the Keldysh contour. In principle, for a coupled e-ph system, one should include processes to all orders in the interaction to calculate self-consistently the different electron Green's functions dressed by the phonons, as well as the phonon Green's functions dressed by the electrons. This is a tremendous task to achieve for realistic systems, and so far it has only been done almost exactly for model systems or within some approximations for atomic or molecular wires. Recent studies have been performed using the so-called self-consistent Born approximation [24, 25, 26, 27], in which the retarded electron self-energy due to e-ph coupling is obtained from the sum of several contributions all written in the following form: $\Sigma^r_{\text{eph},XY}(\omega) \propto i\gamma_0^2 \int d\omega' D^X(\omega - \omega') G^Y(\omega')$, where the superscripts $X, Y \equiv r, >$ represents the different types of Green's functions (retarded r, Keldysh greater $>$) for the electrons (G) and for the phonons (D).

In the following, we work with the undressed phonon Green's functions $D_0(\omega)$ for which the Keldysh greater component is $D_0^>(\omega) = -i2\pi(N(\omega)\delta(\omega + \omega_0) + (N(\omega) + 1)\delta(\omega - \omega_0))$, $N(\omega)$

[1] It should be noted that no polaron shift is obtained if one makes a perturbative expansion of the e-ph coupling.

[2] This is a closed form for a lowest order series expansion of the e-ph self-energy equivalent to the self-consistent Born approximation [24, 25, 26, 27]. In fact the continued fraction expansion of Σ^r_{eph} includes a factor n at each level of the fraction as seen in Eq.(9). Such factors arise from applying the creation (annihilation) phonon operator on the vibrational state $|\chi_{n-1(n)}\rangle$ in a multi-excitation process. The exact series expansion for Σ^r_{eph} includes higher-order terms corresponding to multiple excitations, for example: $\gamma_0^4 \ G^r(\omega - \omega_0) G^r(\omega - 2\omega_0) G^r(\omega - \omega_0)$. A similar result can be obtained by a linked cluster expansion approach.

being the Bose-Einstein distribution function. In the limit of low temperatures, simplifications arise because then $N(\omega) = 0$. Furthermore by using the principle of causality and the analytic properties of G^r in the complex plane, it can be shown that the contribution $\Sigma^r_{\mathrm{eph},rr}(\omega) = -i\gamma_0^2 \int d\omega'/2\pi\ D_0^r(\omega-\omega')G^r(\omega')$ vanishes[3]. The second contribution to the self-energy is given by $i\gamma_0^2 \int d\omega'/2\pi\ D_0^>(\omega-\omega')G^r(\omega')$. At zero temperature, this is exactly the self-energy $\gamma_0^2\ G^r(\omega-\omega_0)$ derived previously in Eq.(14). The final contribution to the self-energy is $\Sigma^r_{\mathrm{eph},r>}(\omega) \propto \int d\omega'(D_0^r(\omega')-D_0^r(\omega=0))G^>(\omega-\omega')$. It involves the greater electron Green's function $G^>$ which provides information about the non-equilibirum density of unoccupied states of the molecule. $G^>$ is related to the corresponding self-energy $\Sigma^> = \Sigma^>_{\mathrm{leads}}+\Sigma^>_{\mathrm{eph}}$ and the retarded and advanced Green's functions $G^{r,a}$ via the kinetic equation $G^> = G^r\Sigma^>G^a$. The terms involving $\Sigma^>_{\mathrm{eph}}$ are intrinsically of higher order in $\mathcal{O}(\gamma_0^2)$ than $\Sigma^r_{\mathrm{eph}}(\omega) = \gamma_0^2\ G^r(\omega-\omega_0)$ and can be neglected for weak e-ph coupling. The other terms involving $\Sigma^>_{\mathrm{leads}}$ are important; however their contributions become small when the electronic level coupled to the vibration is off-resonance with the Fermi levels of the leads (in the limit of zero to small applied bias). This is case for molecular wires having a substantial HOMO-LUMO gap, when the Fermi levels are pinned inside this gap.

So, the multichannel scattering technique takes into account the most important contributions to the e-ph self-energy. There are some terms arising from the Keldysh approach to transport that are not treated in the multichannel technique; however, as mentioned above, the general problem of the non-equilibrium transport is so complex that it has only been solved for model systems and using approximations for the Green's functions and self-energies [23, 24, 25, 26, 27].

Now that we have established how to relate the multichannel scattering technique to other widely used non-perturbative approaches for transport through e-ph coupled systems, we turn to some practical applications of the technique.

Results

In our previous studies on long conjugated molecules [18, 17], we have already shown that the longitudinal optic phonon modes are the most strongly coupled to the injected charges. We have elucidated the mechanisms of charge injection and transport in such molecular wires. The transport is associated with the formation and propagation of polarons in perfectly dimerized (semiconducting) molecular wires [17]. More complex mechanisms arise in the presence of mid-gap states involving the delocalisation of a soliton and polaron-soliton interactions [18].

Here we present new results for models of molecules in relation with recent experiments; namely we consider the effects of the temperature on the conductance peaks around the HOMO-LUMO gap for short molecular wires [34], and we point out the difficulties for understanding the features observed in IETS [5, 6] in terms of single vibration mode analysis. In doing so, we provide a plausible explanation for the temperature dependence of the width and shape of conductance peaks from a model system. More importantly, we show that it is crucial to treat the coupling to all the relevant vibration modes simultaneously, instead of considering one mode at a time, in order to be able to identify the origin of the features in IETS spectra.

Temperature effects on the conductance peaks

Here we consider the experiments performed with a mechanically controlled breakjunction at room temperature and at low temperature ($T \approx 30$K) for polyphenylene-based molecular wires [34]. The conductance curves show a peak just above a region of very low conductance at small bias (which might be a HOMO-LUMO gap or Coulomb gap). At low temperature, the peak is asymmetric with a maximum width of $\sim$125 meV. At room temperature, this peak has a reduced amplitude and is more symmetric with a bell-like shape of maximum width 300 meV. It is clear that such a temperature dependence cannot be explained by the broadening of the

[3]This is always true for electron-hole-symmetric systems. It is also true when the system is not too far from equilibrium.

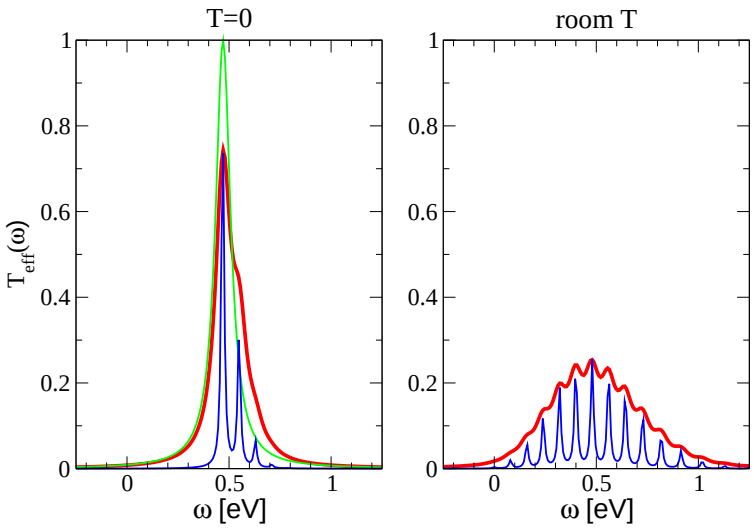

Figure 1: Total effective transmission $T_{\rm eff}$ versus energy ω for the SSSM model ($\epsilon_0 \approx 0.5$ eV, $\omega_0 \approx 80$ meV, $\gamma_0 \approx \omega_0/2$). *Left panel*: Very low temperature limit: the transmission peak (red line) is asymmetric towards higher energy because of the presence of phonon side-bands corresponding to phonon emission. The resonance peak obtained in the absence of e-ph coupling (green line) is symmetric around ϵ_0. *Right panel*: At room temperature, both phonon emission and adsorption processes are available. The transmission peak (red line) is more symmetric around ϵ_0 and its amplitude is reduced. In both panels, the blue lines represent the transmission obtained for a strongly reduced broadening in order to show explicitly the phonon side-bands.

Fermi sea of the electrodes: a broadening over kT is not enough to explain the widening of the conductance peak and its change of shape. We therefore assume that there are fluctuations within the junction or at the molecule-electrode contacts, and that these fluctuations are related to low frequency vibration modes. It is difficult to identify exactly the nature of such modes, so we consider for simplicity a SSSM model in which the single level ϵ_0 is coupled to a low frequency vibration mode ($\omega_0 \approx 80$ meV) via a coupling constant $\gamma_0 \approx \omega_0/2$.

We perform calculations for this model according to the prescriptions given in the previous section at very low temperature and at room temperature. The total effective transmission $T_{\rm eff}(\omega)$ is obtained as the sum of all the elastic and inelastic contributions to the transmission and is shown in Fig. 1 for the zero temperature limit ($kT = 0$) and for room temperature ($kT \approx \omega_0/2$). In the absence of e-ph coupling, the transmission is given by a single symmetric resonance located around ϵ_0, as expected. In the presence of e-ph coupling, the shape of the resonance is modified due to the presence of phonon side-bands. For very low temperatures, the transmission peak is asymmetric towards higher energy. The phonon side-band peaks are located at energies above ϵ_0 because only phonon emission processes are allowed at low temperatures. At room temperature, both phonon emission and absorption processes become possible and the phonon band peaks appear for energies above and below the molecular level.[4] The transmission peak is then more symmetric around ϵ_0. Futhermore, its amplitude is reduced compared to the peak at $T = 0$, as observed experimentally.

[4]This lineshape appears similar to that obtained for very low temperature and very strong coupling [33], but the physics is quite different because absorption processes are important.

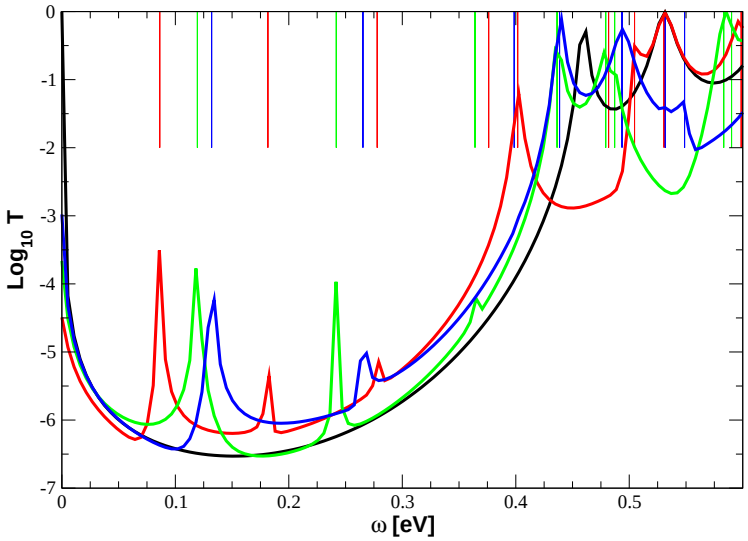

Figure 2: Total effective transmission $T_{\rm eff}$ versus energy ω for a molecular wire of length $N = 155$. The transmission is calculated by including a single vibration modes one at a time. Optic mode $\omega_{\lambda_1} = 112.1$ meV (red line) showing the most important polaron shift, $\omega_{\lambda_2} = 129.9$ meV (green line), $\omega_{\lambda_3} = 136.8$ meV (blue line). The transmission in the absence of e-ph coupling is also shown (black line). The vertical bars represent (for the same color) the eigenvalues of the isolated molecule Hamiltonian including the coupling of the single mode λ to the many molecular levels.

It is interesting that such a simple model provides results in qualitative agreement with the conductance measurements performed in Ref.[34]. Such a mechanism therefore provides a plausible explanation for the temperature dependence of the conductance peaks in molecular junctions, although we cannot rule out other possible explanations such as those given in Refs. [23, 24].

Multi-vibration mode effects

We now consider a more realistic molecular wire built from an odd number N of monomers as obtained from the SSH model. In this case, there is a mid-gap state in the HOMO-LUMO gap. In the following, we couple all the unoccupied π states to the low energy optic modes as in Eq.(4). The actual spatial and frequency structure of these modes is very important in allowing charge to propagate through the molecule—in contrast to previous studies on simpler model systems [13].

As a generalisation of the SSSM model, there will also be phonon side-bands in the transmission. The phonon side-band peaks related to the mid-gap state will appear inside the HOMO-LUMO gap. Such peaks also exist in the absence of the mid-gap state, i.e. for wires of even length N; however, there they are hidden in the background of the resonances from the molecular conduction band.

The transmission curves for a wire of length $N = 155$ in which the molecular levels interact with a single vibration mode one at a time are shown in Fig.2. Several different optic modes ($\omega_{\lambda_1,\lambda_2,\lambda_3} = 112.1$, 129.9, 136.8 meV) are considered. The total effective transmission $T_{\rm eff}$ shows phonon side-band peaks in the HOMO-LUMO gap, separated as expected by the corresponding

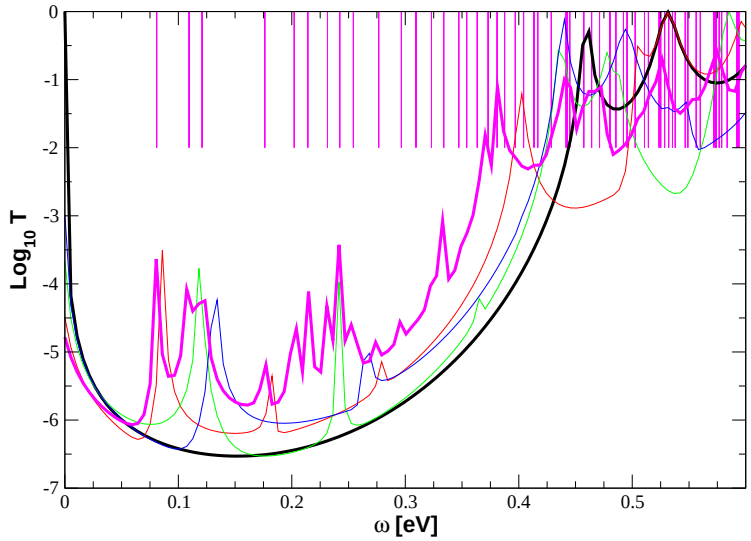

Figure 3: Total effective transmission $T_{\rm eff}$ versus energy ω for a molecular wire of length $N = 155$. The transmission (magenta line) is calculated by including the coupling to the three optic modes shown in Fig.2. New spectroscopic features appear in the transmission. The vertical bars give the eigenvalues of the isolated molecular Hamiltonian with many levels coupled to the three optic modes. The transmission in the absence of e-ph coupling is also shown (black line) as well as the transmission obtained for a coupling to a single mode (thin solid line) as in Fig. 2.

energy ω_λ. Up to small energy shifts due to real part of the self-energies, the peaks in the transmission correspond to the eigenvalues of the coupled e-ph Hamiltonian of the isolated molecule, as shown by the vertical bars in Fig.2. For some eigenvalues, there are no resonances in the transmission. There are several possible reasons for this: (i) the phonon side-band peaks associated to a given electronic transition have an exponentially decaying weight for large numbers of excitation quanta, so some of these peaks may disappear in the tail of other resonances; (ii) there might be destructive quantum interferences for the corresponding process[5]; (iii) the corresponding eigenstates are such that the matrix elements $\langle N|G^r_{ab}|1\rangle$ in Eq.(7) are small or vanishing.

Note that such calculations also reveal which optic phonon mode contributes the most to the polaron shift (shift towards lower energy of the first resonance above the gap due to the e-ph coupling). In the present case, the optic mode of energy $\omega_{\lambda_1} = 112.1$ meV gives the most important polaron shift.

However for realistic molecules, the e-ph coupling matrix is non-diagonal and at the same time the injected charge may couple simultaneously to different vibration modes. Calculations including simultaneous coupling to the three optic modes mentioned above were performed. New spectroscopic information is obtained, as shown in Fig. 3. The transmission is not simply a superposition of the contribution of the three different modes shown in Fig. 2; instead, new peaks appear. These features can be interpreted in terms of quantum interferences between the different elastic and inelastic electron paths as well as in terms of beating effects. All

[5]Such effects appear more often when several electronic levels are coupled simultaneously to several vibration modes.

these features in the transmission correspond to the eigenvalues of the coupled e-ph molecular Hamiltonian H, provided coupling of the many molecular levels to the three different vibration modes is included. A detailed analysis of the origins of such features is beyond the scope of the present paper; however, these effects show that the general form for the e-ph coupling Eq.(4) in realistic systems creates features in the transmission that cannot be obtained in terms of single vibration mode analysis.

This is a very important result when one considers the interpretation of recent IETS experiments in molecular junctions[6]. Our results shown that special care is needed when assigning features in the transmission or the current to specific vibration modes of the molecular junction. Calculations for realistic three-dimensional geometries in molecular junctions are currently under investigation.

References

[1] Kouwenhoven, L.P., Austing, D.G., & Tarucha, S. (2001)*Rep. Prog. Phys.* **64** 701–736.

[2] Emin, D. & Holstein, T. (1976) *Phys. Rev. Lett.* **36** 323–326.

[3] Ho, W. (2002) *J. Chem. Phys.* **117**, 11033-11061.

[4] Park, H., Park, J., Lim, A.K.L., Anderson, E.H., Alivisatos, A.P. & McEuen, P.L. (2000) *Nature* **407**, 57-60.

[5] Kushmerick, J.G., Lazorcik, J., Patterson C.H. & Shashidhar, R. (2004) *Nano Lett.* **4**, 639-642.

[6] Wang, W., Lee, T., Kretzschmar I. & Reed, M.A. (2004) *Nano Lett.* **4**, 643-646.

[7] Yu, L.H., Keane, Z.K., Ciszek, J.W., Cheng, L., Stewart, M.P., Tour, J.M. & Natelson, D. (2004) *Phys. Rev. Lett.* **93**, 266802.

[8] Heeger, A.J. (2001) *Rev. Mod. Phys.* **73**, 681-700.

[9] Persson, B.N.J. & Baratoff A. (1987) *Phys. Rev. Lett.* **59**, 339-342.

[10] Lorente, N. & Persson, M. (2000) *Phys. Rev. Lett.* **85**, 2997-3000.

[11] Todorov, T.N. (1998) *Phil. Mag.* B **77**, 965-73.

[12] Chen, Y.C., Zwolak, M. & Di Ventra, M. (2004) *Nano Lett.* **4**, 1709-1712.

[13] Bonča, J. & Trugman S.A., (1995) *Phys. Rev. Lett.* **75**, 2566-2569.

[14] Ness, H. & Fisher, A.J. (1999) *Phys. Rev. Lett.* **83**, 452-455.

[15] Haule, K. & Bonča, J. (1999) *Phys. Rev. B* **59**, 13087-13093.

[16] Mingo, N. & Makoshi K. (2000) *Phys. Rev. Lett.* **84**, 3694-3697.

[17] Ness, H., Shevlin, S.A. & Fisher, A.J. (1999) *Phys. Rev. B* **63**, 125422.

[18] Ness, H. & Fisher, A.J. (2002)*Europhys. Lett.* **57**, 885-891.

[19] Troisi, A., Ratner, M.A. & Nitzan, A. (2003) *J. Chem. Phys.* **118**, 6072-6082.

[20] Petrov, E.G., May, V. & Hänggi, P. (2004) *Chem. Phys.* **296**, 251-266.

[21] Nitzan, A. (2001) Annu. Rev. Phys. Chem. **52**, 681-750.

[22] Hliwa, M. & Joachim, C. (2002) *Phys. Rev. B* **65**, 085406.

[23] Mii, T., Tikhodeev, S.G. & Ueba, H. (2003) *Phys. Rev. B* **68**, 205406.

[6] Although the total effective transmission is not the differential conductance of the IETS spectra, it contains the same spectroscopic informations of the coupled e-ph system.

[24] Galperin, M., Ratner, M.A. & Nitzan, A. (2004) *Nano Lett.* **4**, 1605-1611.

[25] Pecchia, A., Di Carlo, A., Gagliardi, A., Sanna, S., Frauenhein, T. & Gutierrez, R. (2004) *Nano Lett.* **4**, 2109-2114.

[26] Asai, Y. (2004) *Phys. Rev. Lett.* **93**, 246102.

[27] Frederiksen, T., Brandbyge, M., Lorente, N. & Jauho, A.P. (2004) *Phys. Rev. Lett.* **93**, 256601.

[28] Cornaglia, P.S., Ness, H. & Grempel, D.R. (2004) *Phys. Rev. Lett.* **93**, 147201.

[29] Horsfield, A.P., Bowler, D.R., Fisher, A.J., Todorov, T.N. & Montgomery M.J. (2004) *J. Phys.: Condens. Matter* **16**, 3609-3622.

[30] Cahill, K.E. & Glauber, R.J. (1969) *Phys. Rev.* **177**, 1857-1881.

[31] Wingreen, N.S., Jacobsen, K.W. & Wilkins, J.W. (1989) *Phys. Rev. B* **40**, 11834-11850.

[32] Meir, Y. & Wingreen, N.S. (1992) *Phys. Rev. Lett.* **68**, 2512-2515.

[33] Flensberg, K. (2003) *Phys. Rev. B* **68**, 205323.

[34] Reichert, J., Weber, H.B., Mayor, M. & Löhneysen H.V. (2003) *Appl. Phys. Lett.* **82**, 4137-4139.